EUROPEAN ORGANIZATION FOR NUCLEAR RESEARCH

CERN-EP/81-168
21 December 1981

DETERMINATION OF THE GLUON DISTRIBUTION IN THE NUCLEON FROM DEEP INELASTIC NEUTRINO SCATTERING

H. Abramowicz[1], F. Dydak, J.G.H. de Groot, J. Knobloch, J. May, P. Palazzi, A. Para[1], F. Ranjard, D. Schlatter, J. Steinberger, H. Taureg, W. von Rüden, H. Wahl and J. Wotschack

CERN, Geneva, Switzerland

J. Duda, F. Eisele, H.P. Klasen, K. Kleinknecht, B. Pszola, B. Renk and H.J. Willutzki

Institut für Physik*) der Universität Dortmund, Fed. Rep. Germany

T. Flottmann, C. Geweniger, J. Królikowski[1], J. Rothberg[2] and K. Tittel

Institut für Hochenergiephysik* der Universität Heidelberg, Fed. Rep. Germany

C. Guyot, J.P. Merlo, B. Peyaud, J. Rander, J.P. Schuller and R. Turlay

D.Ph.P.E., CEN-Saclay, France

J.T. He, T.Z. Ruan and W.M. Wu

Institute of High-Energy Physics, Beijing, People's Rep. China

(Submitted to Zeitschrift für Physik)

---

*) Supported by the Bundesministerium für Forschung und Technologie, Bonn, Fed. Rep. Germany.

1) On leave from the Institute for Nuclear Research, Warsaw, Poland.

2) On leave from the Dept. of Physics, University of Washington, Seattle, USA.

ABSTRACT

The observed scaling violations of the nucleon structure functions F_2 and $\bar{q}$ have been analysed in the framework of perturbative QCD to determine the shape and magnitude of the gluon distribution. The data are in good agreement with leading order QCD, and the simultaneous use of F_2 and $\bar{q}$ structure functions permits, for the first time, a reliable determination of the gluon structure function.

1. INTRODUCTION

It is well known that quarks and antiquarks carry only about 50% of the nucleon momentum, the other half being attributed to gluons. Apart from their task of binding the hadrons, gluons are expected to show up directly as elementary hadron constituents in hard hadron-hadron scattering processes such as Drell-Yan μ-pair production, direct photon production, and high-p_T scattering, and in heavy quark production by photons, muons, and neutrinos. It is therefore important to know the gluon distribution in order to be able to make predictions for these reactions. In deep inelastic lepton scattering, gluons do not take part directly in the elementary scattering processes. However, QCD predicts that their interaction with quarks inside the nucleon leads to characteristic scaling violations in the observable structure functions via gluon bremsstrahlung and quark pair production. If the observed scaling violations are predominantly due to QCD effects, the measured Q^2-slopes of the structure functions are directly related to the gluon distribution and can be used to determine its shape and magnitude.

2. DETERMINATION OF STRUCTURE FUNCTIONS F_2 AND $\bar{q}^{\bar{\nu}}$

The present analysis is based on the measurement of the structure functions $F_2(x,Q^2)$ and $\bar{q}^{\bar{\nu}}(x,Q^2) = x(\bar{u}+\bar{d}+2\bar{s})$ by high-energy neutrino and antineutrino interactions in iron, using the CERN-Dortmund-Heidelberg-Saclay (CDHS) detector [1]. The structure function F_2 is measured using narrow-band beam data only, whereas the measurement of $\bar{q}$, which needs high statistics, uses wide-band beam data in addition. In total we use 94,000 neutrino and 25,000 antineutrino charged-current events from narrow-band beams and 35,000 neutrino and 155,000 antineutrino events from wide-band beams. The data selection, extraction of differential cross-sections, and the determination of structure functions will be described in detail in a forthcoming paper [2].

The structure function F_2 is obtained from the sum of neutrino and antineutrino cross-sections, whereas $\bar{q}^{\bar{\nu}}$ is measured by antineutrino scattering at high y:

$$F_2^{\nu N} \equiv x(u+d+s+c+\bar{u}+\bar{d}+\bar{s}+\bar{c})(1+R) =$$

$$= \frac{1+R}{1+(1-y)^2}\left\{\frac{\pi}{MEG^2}\left[\frac{d^2\sigma^{\nu}}{dxdy}+\frac{d^2\sigma^{\bar{\nu}}}{dxdy}\right] - 2F_L(1-y) - 4x\delta - 4xc(1-y)^2\right\} + x(s+\bar{s}+c+\bar{c})(1+R) \tag{1}$$

$$\bar{q}^{\bar{\nu}} \equiv x(\bar{u}+\bar{d}+2\bar{\delta}) =$$

$$= \frac{1}{1-(1-y)^4}\left\{\frac{\pi}{MEG^2}\left[\frac{d^2\sigma^{\bar{\nu}}}{dxdy} - (1-y)^2\,\frac{d^2\sigma^{\nu}}{dxdy}\right] - F_L\left[(1-y) - (1-y)^3\right]\right.$$

$$\left. + (2x\delta - 2xc)\left[(1-y)^2 - (1-y)^4\right]\right\}. \tag{2}$$

Here $F_L = F_2 - 2xF_1$ is the longitudinal structure function related to $R = \sigma_L/\sigma_T = F_L/2xF_1$; u, d, s, c are the up, down, strange, and charmed quark densities in the proton; and $x\delta(x,Q^2)$ is the strange-quark structure function in the nucleon as seen by the weak charged current. Note that in our Q^2-range $x\delta(x,Q^2)$ exhibits a threshold behaviour in contrast to $xs(x,Q^2)$. This is due to the fact that the transition $s \to c$ is Cabibbo favoured and the charmed quark in the final state has a high mass. For the sake of transparency, mass correction terms of the order of Q^2/ν^2, which were included in the analysis, have been omitted in eqs. (1) and (2).

To extract the structure functions $F_2^{\nu N}$ and $\bar{q}^{\bar{\nu}}$ from the measured differential cross-sections we have to know $R = \sigma_L/\sigma_T$, and we need information about the shape and magnitude of charmed and strange sea and the effect of charm threshold. We take $R(x,Q^2)$ from a previous analysis of the narrow-band beam data [3] and $x\delta(x,Q^2)$ from an analysis [4] of opposite sign dimuon data. Since the uncertainties in both quantities are large, the present analysis uses different sets of structure functions $F_2^{\nu N}$ and $\bar{q}^{\bar{\nu}}$ which are extracted under various assumptions about the strange and charmed sea and the magnitude of $R(x,Q^2)$.

Radiative corrections have been applied according to the prescription of De Rújula et al. [5].

3. METHOD OF EXTRACTING THE GLUON STRUCTURE FUNCTION

The Q^2-evolution of the structure functions F_2, $\bar{q}^{\bar{\nu}}$, and the gluon distribution G(x) due to QCD effects are given by the Altarelli-Parisi equations [6]:

$$\frac{dF_2(x,Q^2)}{d\ \ln\ Q^2} = \frac{\alpha_s(Q^2)}{2\pi} \int_x^1 \left[P_{qq}\left(\frac{x}{z}\right) F_2(z,Q^2) + 2N_{F_2} P_{gq}\left(\frac{x}{z}\right) G(z,Q^2) \right] \frac{xdz}{z^2} \qquad (3a)$$

$$\frac{d\bar{q}(x,Q^2)}{d\ \ln\ Q^2} = \frac{\alpha_s(Q^2)}{2\pi} \int_x^1 \left[P_{qq}\left(\frac{x}{z}\right) \bar{q}(z,Q^2) + N_{\bar{q}} P_{gq}\left(\frac{x}{z}\right) G(z,Q^2) \right] \frac{xdz}{z^2} \qquad (3b)$$

$$\frac{dG(x,Q^2)}{d\ \ln\ Q^2} = \frac{\alpha_s(Q^2)}{2\pi} \int_x^1 \left[F_2(z,Q^2) P_{qg}\left(\frac{x}{z}\right) + P_{gg}\left(\frac{x}{z}\right) G(z,Q^2) \right] \frac{xdz}{z^2} \ . \qquad (3c)$$

Here N_{F_2} and $N_{\bar{q}}$ are the number of flavours which contribute to the evolution of the F_2 and $\bar{q}$ structure functions, respectively. Our standard set of structure functions has $N_{F_2} = N_{\bar{q}} = 4$. The splitting functions P_{ij} are known (in leading order) and the structure functions F_2 and $\bar{q}$ are measured. Given the structure functions $F_2(x,Q_0^2)$ and $\bar{q}(x,Q_0^2)$ at some Q_0^2, and their Q^2-evolution at this Q_0^2, we can determine

$$\alpha_s(Q_0^2) = \frac{12\pi}{25\ \ln\ (Q_0^2/\Lambda_{LO}^2)}$$

(or the scale parameter Λ_{LO}) and the unknown gluon distribution $G(x,Q_0^2)$ on the basis of eqs. (3a) and (3b). The predictions of the Altarelli-Parisi equations for the Q^2-evolution of F_2 and $\bar{q}$ are compared directly to the measured slopes of our structure function set I (table 1) in figs. 1a,b for $Q_0^2 = 4.5\ GeV^2/c^2$, where the contributions due to gluon bremsstrahlung and gluon pair production are given separately. The curves shown correspond to the best QCD fit to the data as described below. The data are not precise enough to measure the slopes locally (in a small Q^2 range). The data points in fig. 1 are therefore obtained by linear fits to F_2 in ln ln Q^2 for fixed x using all available Q^2 values. This procedure is only a rough approximation to the expected QCD behaviour, such that the data points do not have to agree completely with the correct QCD solution. However, they show very well that significant scaling violations are observed both for F_2 and $\bar{q}$, and their pattern is in good agreement with the QCD prediction. A

measurement of F_2 alone does not allow a good simultaneous determination of $\alpha_s(\Lambda)$ and the gluon distribution since both are very strongly correlated. If α_s were increased in fig. 1a, the negative bremsstrahlung contribution to $dF_2/d \ln Q^2$ would become larger than the observed scaling violations at large x. This could be compensated by the positive contribution of a broader gluon distribution. However, the additional measurement of $\bar{q}^{\bar{\nu}}$, whose scaling violations are also very strongly linked to the gluon distribution, allows us to decouple Λ and the width of the gluon distribution. In particular, the convolution $P_{gq} \otimes G(x)$ has to be zero where no antiquarks are observed, i.e. for $x \gtrsim 0.45$.

The quantitative confrontation of the data with QCD is based on the simultaneous numerical integration of eqs. (3a)-(3c) using leading-order expressions for α_s and the splitting functions*). Equations (3a)-(3c) constitute a system of coupled ordinary differential equations (one equation for each measured value of x and each structure function). As boundary conditions the structure functions are parametrized for $Q^2 = Q_0^2$ in the following way:

$$\begin{aligned} F_2(x,Q_0^2) &= a_2(1+b_2x)(1-x)^{c_2} \\ G(x,Q_0^2) &= a_g(1+b_gx)(1-x)^{c_g} \\ \bar{q}(x,Q_0^2) &= a_q(1-x)^{c_q} \ . \end{aligned} \tag{4}$$

The shape parameters a_i, b_i, c_i and the parameter Λ_{LO} are then determined by a least squares fit to the data. The distribution $G(x,Q_0^2)$ cannot be compared directly with the data, in contrast to F_2 and $\bar{q}$. It is therefore important to choose a reasonable parametrization. Our choice (4) is motivated by counting rule predictions at large x. In addition, it allows for substantial variations in shape at small x.

The numerical solution of the Altarelli-Parisi equations has the advantage that it can make full use of all available data and that it depends only weakly on unmeasured kinematical regions at large x. This is because the convolution $\int_x^1 P_{qq}F_i(z) \cdot x/z^2 dz$ gets contributions mainly from z values which are near to x where the structure function is measured.

---

*) The method has been introduced by L.F. Abbott and M. Barnett. We use a modified version of their program.

4. FIT RESULTS

Our standard set of structure functions (set I) [2] is obtained from eqs. (1) and (2) assuming that the strange sea and $x(\bar{u}+\bar{d})$ have the same x distributions but that xS is suppressed by a factor $2(S-c)/(\bar{u}+\bar{d}) = 0.4$. This assumption is based on the measurement of opposite-sign dimuon events [4]. It implies that no correction for charm threshold is done and the contribution of the charmed sea is small. The value of $R = \sigma_L/\sigma_T$ has been fixed to $R = 0.1$ in agreement with the published result [3]. In addition, a small correction has been applied to correct for the non-isoscalarity of the iron nucleus.

In the QCD fits we have used all data points for F_2 and $\bar{q}$ with $Q^2 > 2$ GeV$^2/c^2$ and the invariant hadron mass squared $W^2 > 11$ GeV^2. The latter cut is imposed to avoid the kinematical region where higher-twist contributions might be important and where second-order and non-leading corrections are substantial. Target mass corrections are applied according to the prescription of Barbieri et al. [7]. We have also included a propagator term with a mass $m_W = 80$ GeV.

In a first step we enforce the energy momentum sum rule, i.e. the total gluon and quark momenta have to add up to the nucleon momentum. We obtain the following fit results for structure function set I at $Q_0^2 = 5$ GeV$^2/c^2$:

Structure function set I: $N_{F_2} = 4$, $N_{\bar{q}} = 4$

$$\Lambda_{LO} = 0.18 \pm 0.02$$

$\langle F_2\rangle_2 = 0.45 \pm 0.02$	$\langle x\rangle_{F_2} = 0.25 \pm 0.01$	$Q_0^2 = 5$ GeV$^2/c^2$
$\langle \bar{q}\rangle_2 = 0.055 \pm 0.002$	$\langle x\rangle_{\bar{q}} = 0.095 \pm 0.004$	$\chi^2/DF = 209/196$
$\langle G\rangle_2 = 1 - \langle F_2\rangle_2$	$\langle x\rangle_{glue} = 0.16 \pm 0.012$	

Here $\langle F_i\rangle_2$ and $\langle x\rangle_{F_i}$ are the integral and the average value of x for the structure function F_i, respectively, and the errors are purely statistical. This QCD fit describes the observed scaling violations very well, as can be seen in figs. 1a,b and in figs. 2a,b, which show the structure functions F_2 and $\bar{q}$ versus Q^2 for all x-bins compared with the result of this fit. The correlation between Λ and the

width of the gluon distribution is small. The obtained shape of the gluon distribution is displayed in figs. 3a,b for two values of Q^2 and compared with F_2 and $\bar{q}$. It should be noted that the gluon distribution is determined independently at only one value of Q_0^2. It can then be calculated for every other value of Q^2 using the evolution equations. A simple parametrization including the Q^2-dependence is given in the Appendix.

The validity of the energy momentum sum rule can be tested by leaving also the normalization factor for $G(x,Q_0^2)$, a_g, as a free parameter in the fit. At $Q_0^2 = 5\ GeV^2/c^2$ we obtain

$$\langle G \rangle_2 = 0.55 \pm 0.11 \ , \qquad (5)$$

in good agreement with the expectation: $1 - \langle F_2 \rangle = 0.55$. Alternatively, assuming again the energy momentum sum rule, we can check the number of effective flavours by leaving N_{F_2} and $N_{\bar{q}}$ in eqs. (3a) and (3b) as free parameters. We obtain $N_{F_2} = 4.4 \pm 0.4$ and $N_{\bar{q}} = 3.8 \pm 0.5$, which is well compatible with the expectation.

The structure function set I has also been used to study some systematic dependences. Target mass corrections give a negligible effect in this range of W^2. We note that the choice of Q_0^2 is not completely free if we stick to the gluon parametrization of eq. (5). This specific form is not able to describe the very steep rise of the gluon distribution at large Q_0^2 (as shown in fig. 3b). If it were enforced for a $Q_0^2 \gtrsim 15\ GeV^2/c^2$, the gluon distribution would become negative at low values of Q^2. For the same reason the simple assumption $G(x,Q_0^2) \sim (1-x)^P$, which is often found in the literature, can only hold in an even more limited Q_0^2-range.

The above determination of the gluon distribution and of Λ_{LO} is valid if the observed scaling violations are only due to QCD effects. There are at least two other known effects which give rise to scaling violations: i) the charm threshold for the transitions $s \to c$ and $d \to c$, and ii) the uncertainty in the magnitude and Q^2-dependence of $R = \sigma_L/\sigma_T$. Both effects have been studied systematically. With the present knowledge they contribute a substantial uncertainty to the measured

slopes of $\bar{q}$. In the following fits we have therefore no longer used the slopes of $\bar{q}$, but only require that $\bar{q}$ is close to zero at large x within the well-established experimental limits. This requirement still gives a very good constraint on the width of the gluon distribution. The effect of R on F_2 is rather small, within the experimental uncertainties. The threshold for the charm production from the strange sea, however, contributes substantially to the slopes of F_2 at small x. We have evaluated two different sets of structure functions F_2' in order to estimate the effect on the gluon distribution and Λ_{LO}. The effect of charm threshold has been corrected using the slow rescaling model [8] with two values of the charm mass and the amount of strange sea:

Structure function set II : m_c = 1.5 GeV ; $2s/(\bar{u}+\bar{d}) = 0.5$

Structure function set III: m_c = 1.8 GeV ; $2s/(\bar{u}+\bar{d}) = 1$

} $N_{F_2} = 3$, $R = 0.1$

Both assumptions are compatible with the data on opposite-sign dimuons [4]. The charmed sea has been set to zero for $Q_0^2 = 1\ GeV^2/c^2$, and its Q^2-evolution has been calculated using the QCD equations for the evolution of $xc(x,Q^2)$, F_2, and G, where $F_2(x,Q_0^2)$ and $G(x,Q_0^2)$ have been fixed to the results of fit I. This charmed sea was then subtracted from the expression in eq. (1), leading to a very small correction. The remaining structure function F_2' has only three flavours. We believe that the three data sets give a conservative estimate of the effects due to charm threshold and the amount of strange and charmed sea. The results of the fit to all three data sets are summarized in table 1.

5. CONCLUSIONS

The uncertainties related to the strange and charmed sea and to $R = \sigma_L/\sigma_T$ have only a moderate effect on the results of the present analysis. The value of Λ_{LO} is remarkably stable and in good agreement with the results of a QCD analysis of the non-singlet structure functions xF_3 [9] with $\Lambda_{LO} = 0.2\ ^{+\ 0.15}_{-\ 0.10}$ GeV. The gluon distributions from the fits to all three structure function sets are compared in fig. 4 for $Q_0^2 = 5\ GeV^2/c^2$. It can be seen that the shape and magnitude of G(x)

are only moderately affected by the uncertainties due to charm threshold and the magnitude of strange and charmed sea. Actually this is not too surprising since the integral of $G(x,Q^2)$ is well constrained by the energy momentum sum rule, and the width by the absence of antiquarks at large x. Higher-twist contributions are not expected to give large effects at small x, i.e. in the gluon region. They may, however, be present at large x and affect the result through a change of Λ_{LO}. An analysis [9] of the present data at all W^2 in combination with SLAC e-d data indicates that higher-twist contributions for $W^2 > 11$ GeV^2 are most likely small. We conclude that the combined analysis of F_2 and $\bar{q}$ has provided a reliable measurement of the gluon distribution.

Acknowledgements

We thank M. Barnett for making his fitting program available to us and for useful discussions.

APPENDIX

PARAMETRIZATION OF $G(x,Q^2)$

The structure function for the gluons $G(x,Q_0^2)$ and for the quarks $F_2(x,Q_0^2)$ have been determined in the QCD fits at a reference value $Q_0^2 = 5\ GeV^2/c^2$. For the structure function set I we found:

$$\left.\begin{aligned} G(x) &= 2.62 \times (1+3.5x)(1-x)^{5.9} \\ F_2(x) &= 1.10 \times (1+3.7x)(1-x)^{3.19} \end{aligned}\right\} \text{ for } Q_0^2 = 5\ GeV^2/c^2 \ .$$

The Q^2-evolution of the gluon distribution can then be obtained by the numerical integration of the Altarelli-Parisi equations (3a) and (3c).

In order to facilitate applications, we have parametrized $G(x,Q^2)$ as given by this numerical integration, using the functional dependence

$$G(x,Q^2) = a(1+bx^c)(1-x)^d(Q^2)^e + f\ e^{-(gx+hx^3)} \ ,$$

where the parameters a, b, c, d, e, f, g, and h are Q^2-dependent. This parametrization is entirely *ad hoc*, i.e. it has no theoretical basis. We find:

$$\begin{aligned} a &= 2.616 + 3.99s + 4.46s^2 \\ b &= 3.5 - 6.83s + 80s^2 \\ c &= 1 + 0.806s \\ d &= 5.9 + 40s + 84.2s^2 - 64s^3 \\ e &= (-0.033 - 0.28x + 59.1x^2)(s-s^2) \\ f &= 5.16s - 0.955s^2 \\ g &= -0.48 + 12.2s + 0.38s^2 \\ h &= 29.72 - 32.4s \ , \end{aligned}$$

where

$$s = \ln\left[\frac{\ln\ (Q^2/0.04)}{\ln\ (5/0.04)}\right] .$$

This parametrization approximates the QCD fit to the structure function set I and is reasonably good for $Q^2 > 2$ GeV$^2/c^2$ and energy transfer $\nu < 2 \times 10^5$ GeV. It should be noted that apart from the uncertainties in shape which can be estimated from table 1 and fig. 4, the structure function $G(x,Q^2)$ has also a scale error of ±6% due to the uncertainty in the absolute neutrino cross-sections.

REFERENCES

[1] M. Holder et al. (CDHS Collaboration), Nucl. Instrum. Methods 148, 235 (1978).

[2] H. Abramowicz et al. (CDHS Collaboration), Neutrino and antineutrino charged-current inclusive scattering in iron in the energy range $20 < E_{\nu,\bar{\nu}} < 300$ GeV, in preparation.

[3] H. Abramowicz et al., A measurement of the ratio of longitudinal and transverse structure functions in neutrino interactions between 30 and 200 GeV, submitted to Physics Letters.

[4] J. Knobloch et al. (CDHS Collaboration), New results on dimuons from CDHS, *in* Proc. Neutrino '81 Conf., Hawaii, 1981.

B. Peyaud et al. (CDHS Collaboration), New results on opposite-sign and same-sign dimuons produced by neutrinos and antineutrinos at high energies, *in* Proc. EPS Int. Conf. on High-Energy Physics, Lisbon, 1981.

[5] A. De Rújula et al., Nucl. Phys. B154, 394 (1979).

[6] G. Altarelli and G. Parisi, Nucl. Phys. B126, 298 (1979).

[7] R. Barbieri et al., Nucl. Phys. B117, 50 (1976).

[8] R.M. Barnett, Phys. Rev. D 14, 70 (1976).

[9] F. Eisele et al. (CDHS Collaboration), New results from the CDHS experiment, *in* Proc. Neutrino '81 Conf., Hawaii, 1981.

Table 1

Results of LO QCD-fits to different sets of structure functions.
Target mass corrections are included. $Q^2 > 2\ GeV^2/c^2$, $W^2 > 11\ GeV^2$.

Structure function	Assumptions about s(x), c(x)	Fit results	χ^2/DF
I) F_2, $\bar{q}$ all x	No threshold effect. $2(s-c)/(\bar{u}+\bar{d}) = 0.4$.	$\Lambda_{LO} = (0.18 \pm 0.02)$ GeV $G(x,Q_0^2 = 5) = 2.62(1+3.5x)(1-x)^{5.9\pm0.5}$	209/196
II) F_2' $\bar{q}$ for x > 0.3	$c(x) = 0$ for $Q^2 = 1\ GeV^2/c^2$. $2s/(\bar{u}+\bar{d}) = 0.5$. Slow rescaling with $m_c = 1.5$ GeV.	$\Lambda_{LO} = (0.20 \pm 0.02)$ GeV $G(x,Q_0^2 = 5) = 2.86(1+2.8x)(1-x)^{6.3\pm0.8}$	166/137
III) F_2' $\bar{q}$ for x > 0.3	$c(x) = 0$ for $Q^2 = 1\ GeV^2/c^2$. $2s/(\bar{u}+\bar{d}) = 1$. Slow rescaling with $m_c = 1.8$ GeV.	$\Lambda_{LO} = (0.206 \pm 0.02)$ GeV $G(x,Q_0^2 = 5) = 2.98(1+2.84x)(1-x)^{6.65\pm0.9}$	173/137

Figure captions

Fig. 1 : Slope of structure function versus x for $Q^2 = 4.5\ GeV^2/c^2$. The dashed lines show the contributions due to gluon bremsstrahlung and gluon pair production; the solid lines are the sum of both contributions. These lines correspond to the QCD fit to structure function set I of table 1. The data points are obtained from linear fits to $F(x,Q^2)$ versus ln ln Q^2.

a) Slope for the structure function $F_2^{\nu N}$.

b) Slope for the structure function $\bar{q}^{\bar{\nu}}$.

Fig. 2 : The measured structure functions (set I) versus Q^2 for different bins in x. The solid lines are the result of the leading-order QCD fit.

a) Structure function $F_2^{\nu N}(x,Q^2)$.

b) Structure function $\bar{q}(x,Q^2)$.

Fig. 3 : Gluon distribution G(x), $F_2(x)$, and $2\bar{q}(x)$ for fixed Q^2 as obtained from a leading-order QCD fit to F_2 and $\bar{q}$.

a) $Q^2 = 4.5\ GeV^2/c^2$. Also shown are the $\pm 1\sigma$ bands for G(x) and the measurements of F_2 and $\bar{q}$ projected to this value of Q^2 along the QCD fit.

b) $Q^2 = 22.5\ GeV^2/c^2$.

Fig. 4 : Gluon distributions at $Q_0^2 = 5\ GeV^2/c^2$ for the fits to the three different structure function sets of table 1.

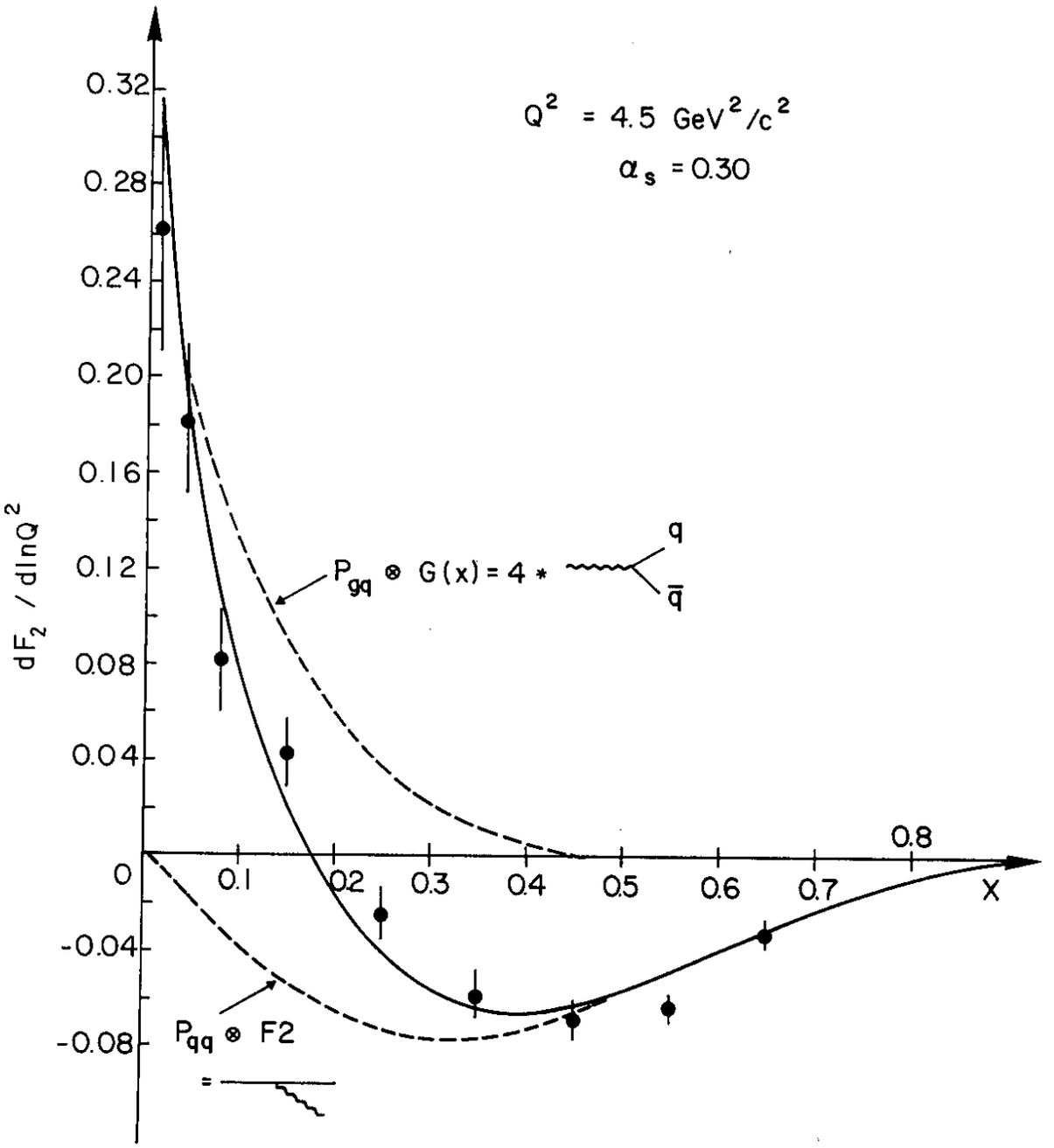
$Q^2 = 4.5\ GeV^2/c^2$
$\alpha_s = 0.30$
$dF_2 / d\ln Q^2$
0.32
0.28
0.24
0.20
0.16
0.12
0.08
0.04
0
-0.04
-0.08
0.1
0.2
0.3
0.4
0.5
0.6
0.7
0.8
X
$P_{qg} \otimes G(x) = 4 *$
q
$\bar{q}$
$P_{qq} \otimes F2$
=

Fig. 1 a)

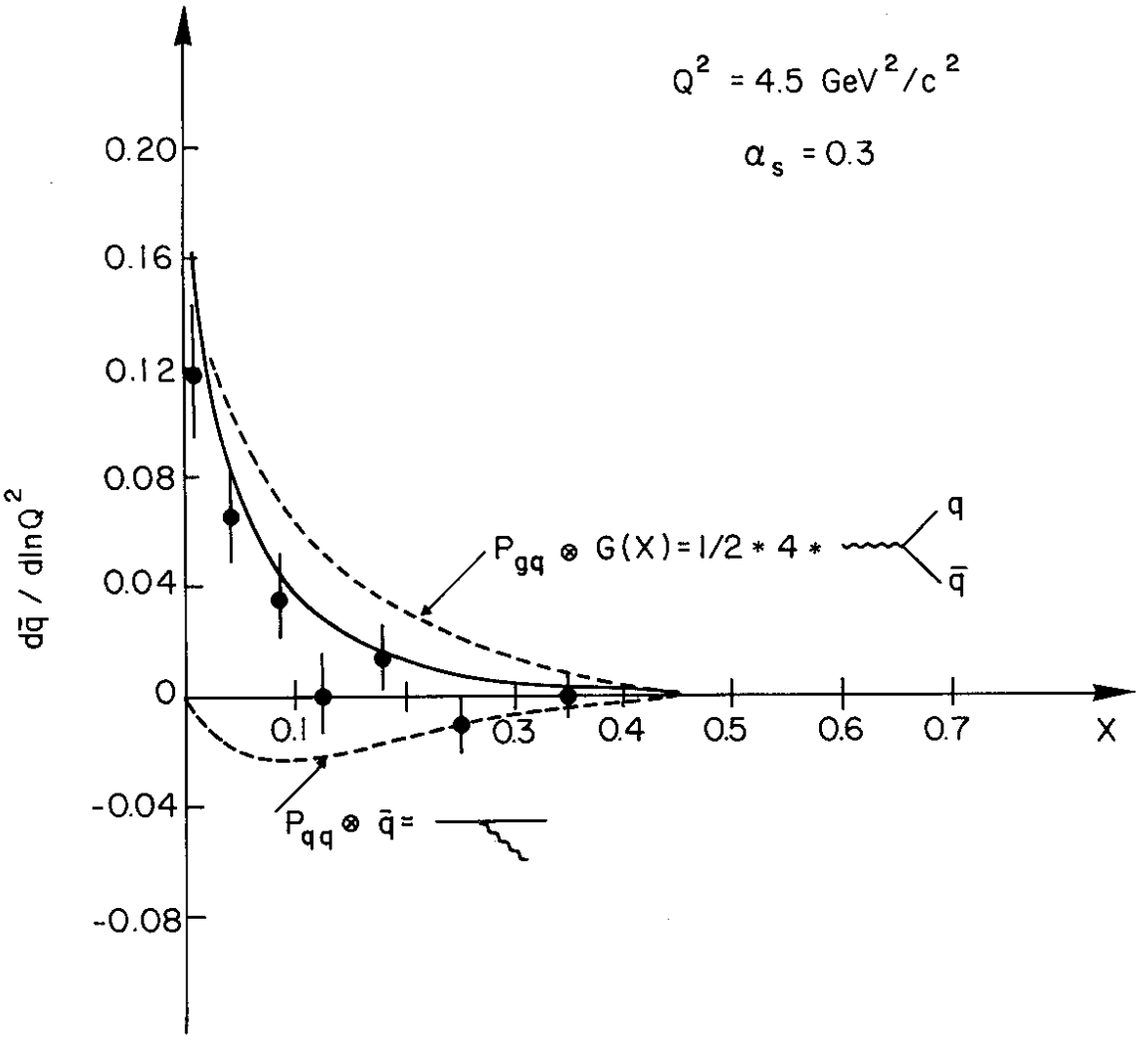
$Q^2 = 4.5\ GeV^2/c^2$
$\alpha_s = 0.3$
0.20
0.16
0.12
0.08
0.04
0
-0.04
-0.08
0.1
0.3
0.4
0.5
0.6
0.7
X
$d\bar{q} / d\ln Q^2$
$P_{gq} \otimes G(X) = 1/2 * 4 *$
q
$\bar{q}$
$P_{qq} \otimes \bar{q} =$

Fig. 1 b)

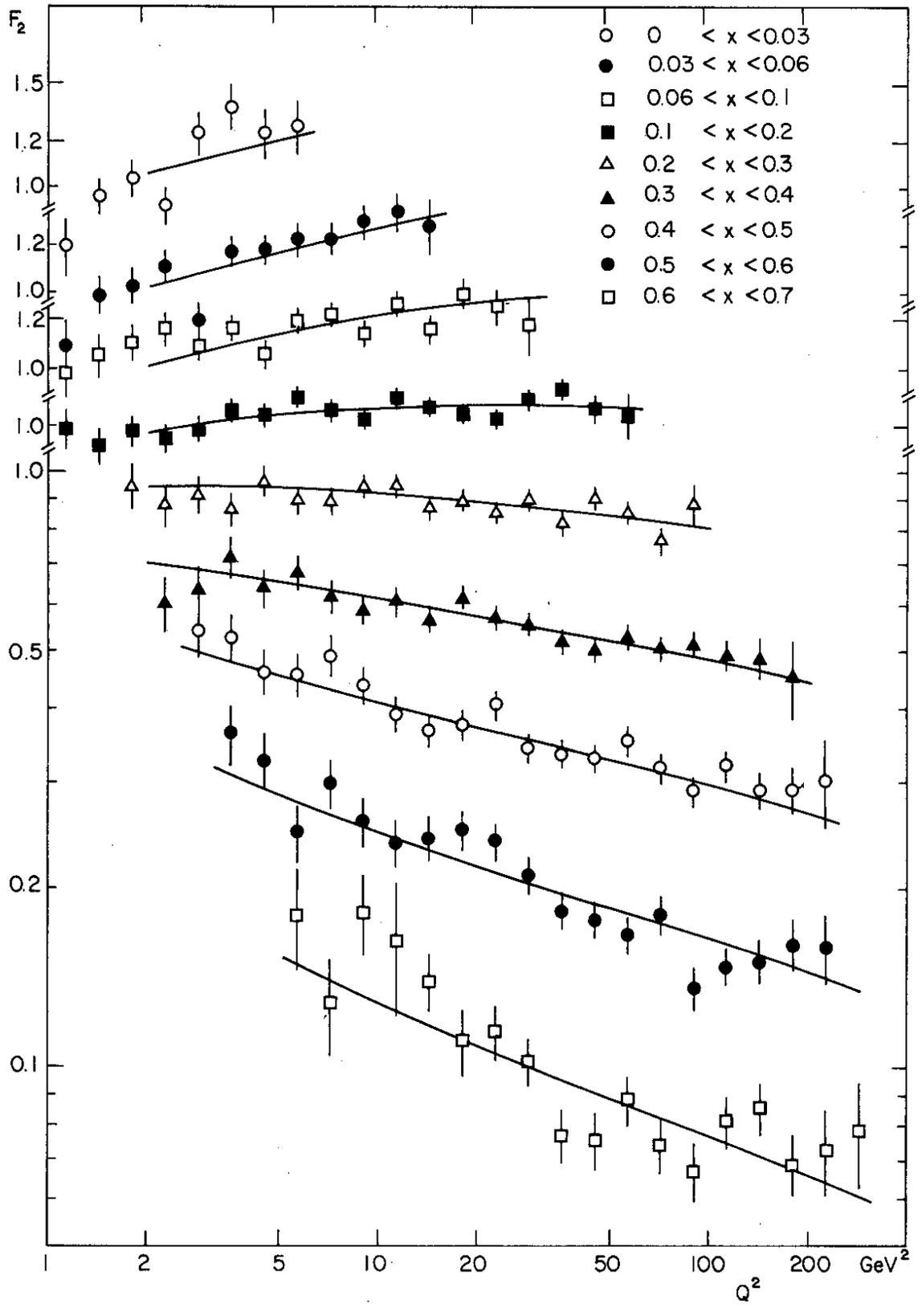
F_2
0 < x <0.03
0.03 < x <0.06
0.06 < x <0.1
0.1 < x <0.2
0.2 < x <0.3
0.3 < x <0.4
0.4 < x <0.5
0.5 < x <0.6
0.6 < x <0.7
1.5
1.2
1.0
1.2
1.0
1.2
1.0
1.0
0.5
0.2
0.1
1
2
5
10
20
50
100
200
GeV^2
Q^2

Fig. 2 a)

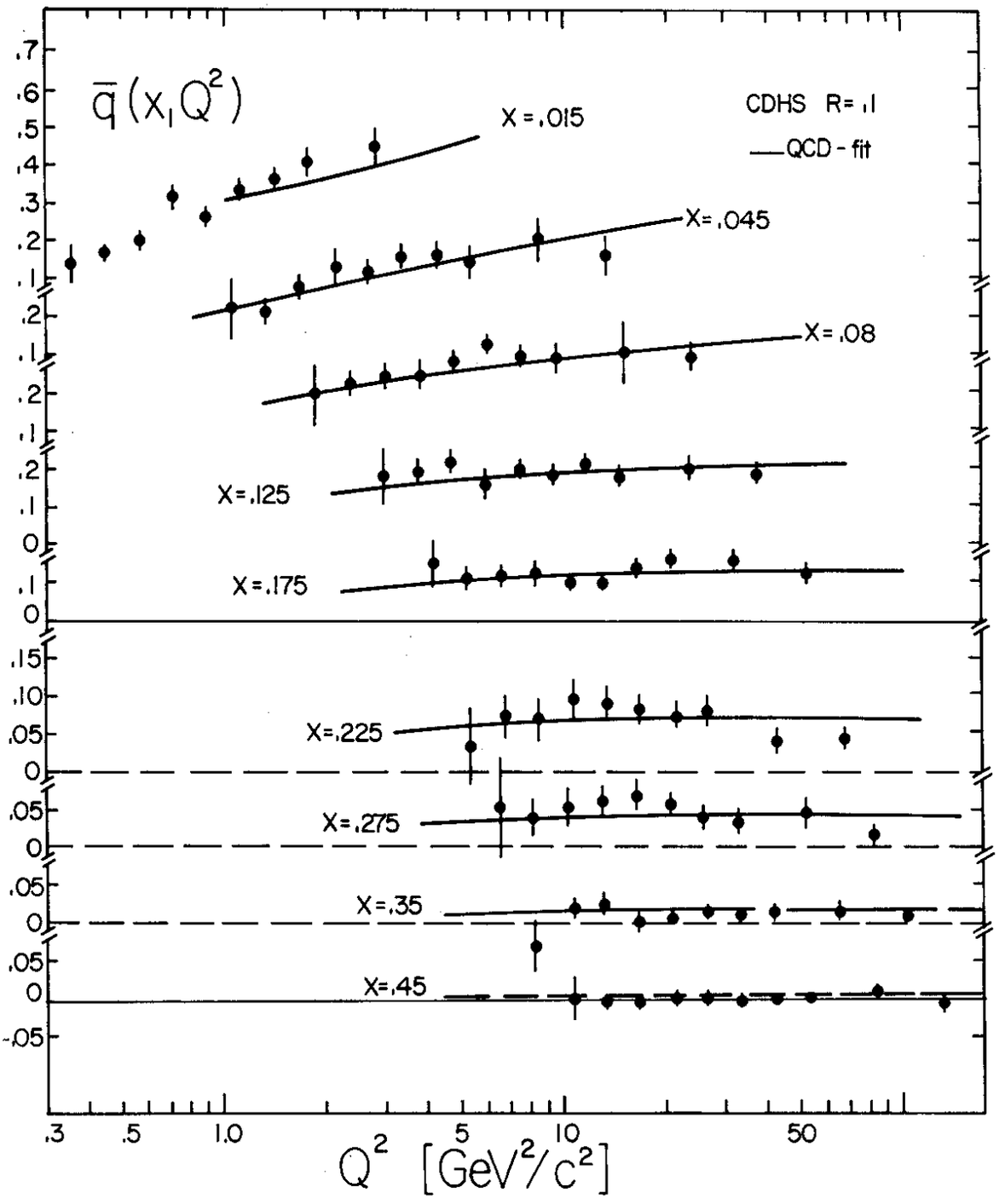
$\bar{q}(x, Q^2)$
CDHS R=.1
—QCD - fit
X=.015
X=.045
X=.08
X=.125
X=.175
X=.225
X=.275
X=.35
X=.45
Q^2 [GeV^2/c^2]

Fig. 2 b)

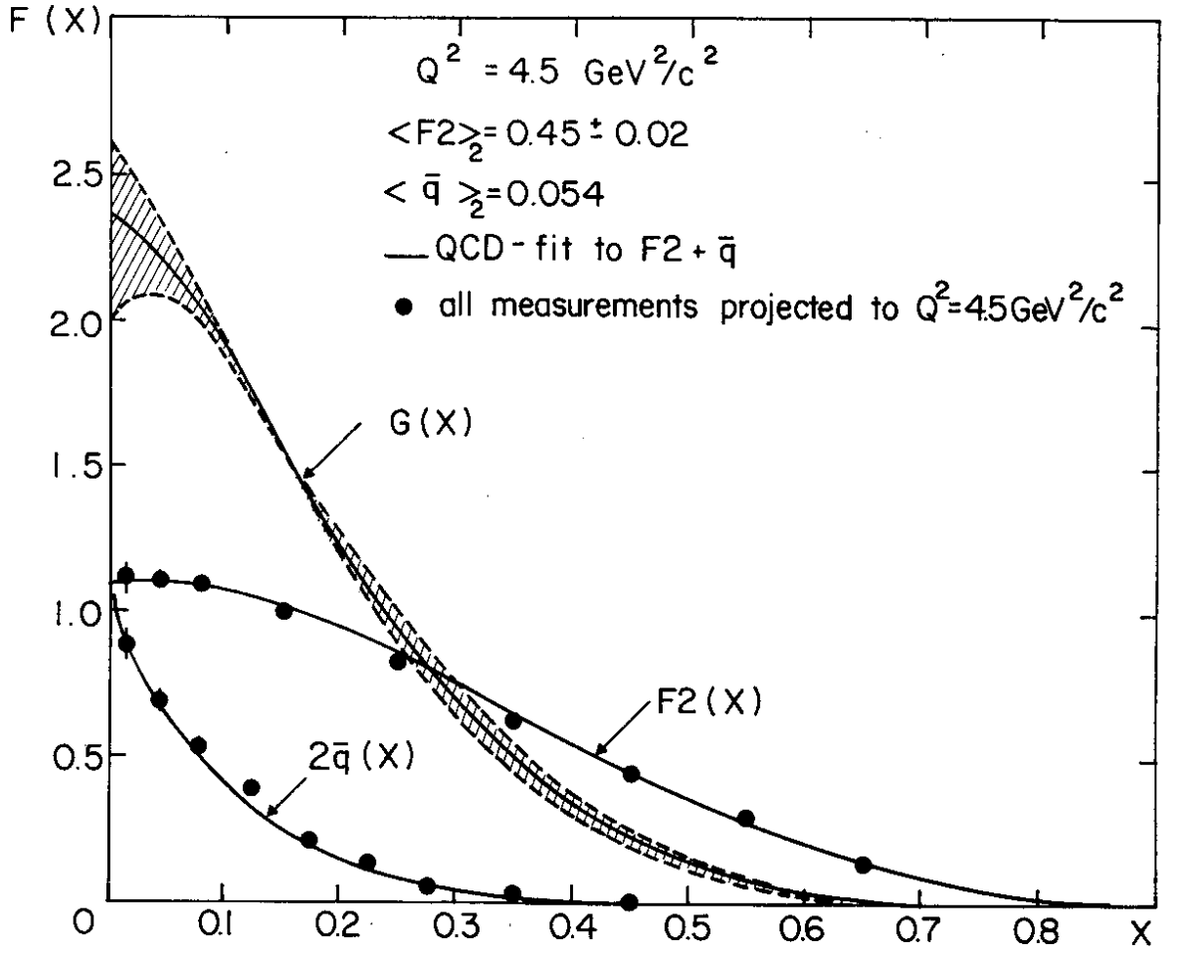
F (X)
Q^2 = 4.5 GeV^2/c^2
<F2>$_2$= 0.45 ± 0.02
< $\bar{q}$ >$_2$=0.054
QCD - fit to F2 + $\bar{q}$
all measurements projected to Q^2=4.5GeV^2/c^2
G(X)
F2(X)
2$\bar{q}$(X)
2.5
2.0
1.5
1.0
0.5
0
0.1
0.2
0.3
0.4
0.5
0.6
0.7
0.8
X

Fig. 3 a)

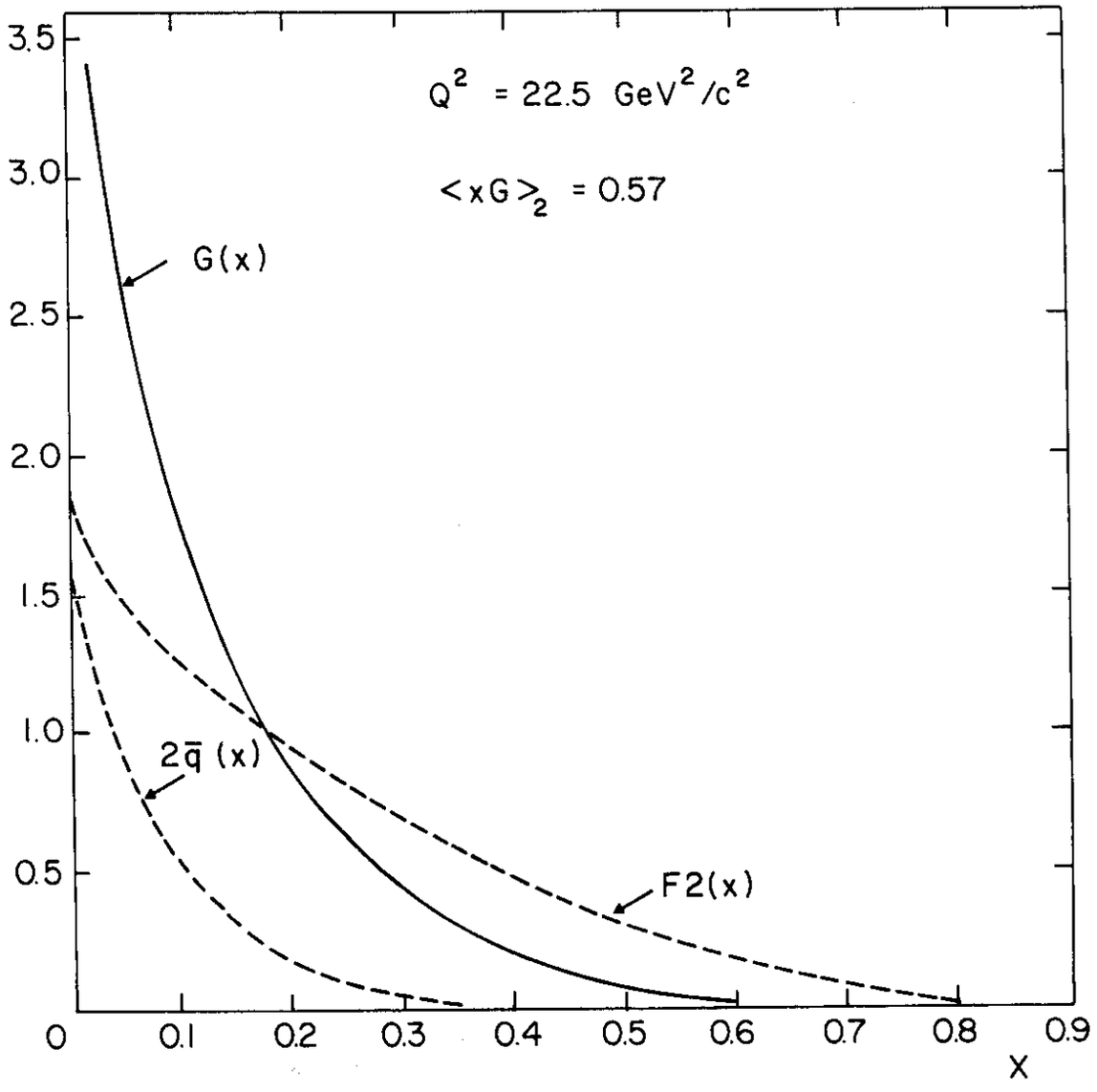
$Q^2 = 22.5\ GeV^2/c^2$
$\langle xG \rangle_2 = 0.57$
G(x)
$2\bar{q}$ (x)
F2(x)
3.5
3.0
2.5
2.0
1.5
1.0
0.5
0
0.1
0.2
0.3
0.4
0.5
0.6
0.7
0.8
0.9
X

Fig. 3 b)

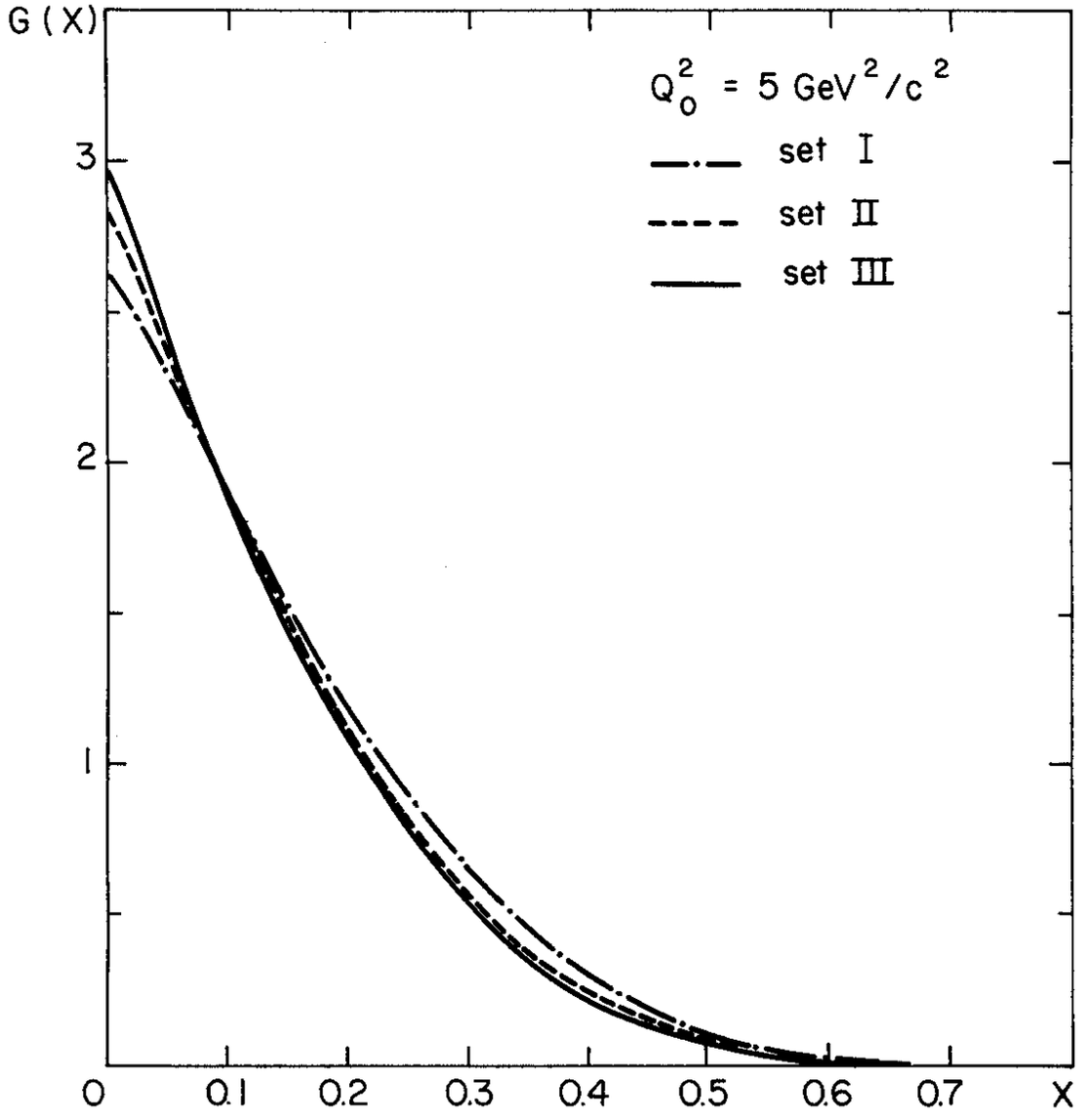

Fig. 4